Journal of Power Sources 221 (2013) 134–140

Contents lists available at SciVerse ScienceDirect

Journal of Power Sources

journal homepage: www.elsevier.com/locate/jpowsour

Effect of diffusion layers fabricated with different fiber diameters on the performance of low temperature proton exchange membrane fuel cells

Chih-Jung Hung [a], Ching-Han Liu [b,*], Tse-Hao Ko [a], Wei-Hung Chen [a], Shu-Hui Cheng [c], Wan-Shu Chen [c], Alan Yu [d], A.M. Kannan [b]

[a] Department of Materials Science and Engineering, Feng Chia University, Taichung 40723, Taiwan
[b] Department of Engineering Technology, Arizona State University, Mesa, AZ 85212, USA
[c] Materials and Chemical Research Laboratories, Industrial Technology Research Institute, Hsinchu 30071, Taiwan
[d] Research and Development Center, Bio-medical Carbon Technology Co., Ltd., Taichung 40755, Taiwan

HIGHLIGHTS

- A new material for GDL precursor is introduced.
- FEP and phenolic resin distributions for PAN fiber felt.
- Diameter of PAN fiber, concentration of phenolic resin and FEP are related to permeability.
- Fuel cell operation has been influenced by the permeability.

ARTICLE INFO

Article history:
Received 6 August 2012
Accepted 7 August 2012
Available online 22 August 2012

Keywords:
Fuel cell
Gas diffusion layer
Carbon fiber paper
Carbon fiber felt
Carbonization
Fiber diameter

ABSTRACT

This study discusses the relationship between performance and carbon fiber diameter (400 nm–1 μm) in fuel cells employing carbon fiber paper produced from PAN fiber felt, and also examines the effect of carbon fiber paper thickness, air permeability, porosity, and surface resistivity on performance. The researchers fabricate gas diffusion layers (GDLs) with a small carbon fiber diameter from PAN fiber employing the two processes of stabilization and carbonization, and investigate the relationship between fiber diameter and air permeability in the gas diffusion layer material. Carbon fiber paper made in this study is left as is or impregnated with 10 wt% phenolic resin or FEP. When the tested area is 25 cm^2, the test temperature 40 °C, and the carbon fiber paper impregnated with 10 wt% phenolic resin, the paper has a fiber diameter of 1 μm and an air permeability is 29 $cm^3\ cm^{-2}\ s^{-1}$, and a test fuel cell yields 997 mA cm^{-2} at a load of 0.5 V. Carbon fiber paper impregnated with 10 wt% FEP has a smaller carbon fiber diameter of 400 nm and an air permeability of only 1 $cm^3\ cm^{-2}\ s^{-1}$; a test fuel cell made with this material yields 683 mA cm^{-2} at a load of 0.5 V.

1. Introduction

Proton exchange membrane fuel cells (PEMFCs) are considered to be superior to other fuel cell systems in vehicle applications due to their higher efficiency and power density and lower operating temperature and noise [1–4]. Gas diffusion layers (GDLs), which provide a channel for the transport of fuel and the transmission of current in PEMFCs, are typically made of carbon fiber paper or carbon fabric, and the composition of a GDL can significantly affect PEMFC performance [5].

Carbon has the advantages of high conductivity and resistance to corrosion, and is well suited to the environment inside a PEMFC. Graphitization of carbon fiber at a temperature of up to 1800 °C increases the conductivity of the fiber while reducing the hydrophobicity of surface functional groups on the fibers [6,7]. When carbon fiber is used to produce a GDL, generally employing a heat treatment temperature in excess of 1400 °C, the different carbon structures obtained employing different carbonization methods can affect the performance of the resulting PEMFC [8]. The production of carbon fiber with good electrical conductivity from polyacrylonitrile (PAN) fiber requires three steps: stabilization, with a temperature range of 200–300 °C, carbonization, at a temperature of approximately 1000 °C in an inert gas such as nitrogen, and graphitization, which requires heating to 1500–3000 °C under controlled conditions [11–18]. While carbon fiber

* Corresponding author. Tel.: +1 480 257 0992.
E-mail address: wowbabytw@gmail.com (C.-H. Liu).

0378-7753/$ – see front matter © 2012 Elsevier B.V. All rights reserved.
http://dx.doi.org/10.1016/j.jpowsour.2012.08.030

fabric is prone to warping and shrinking in fuel cells, carbon fiber paper offers an excellent stability. Moreover, the addition of phenolic resin to the carbon fiber paper can improve PEMFC performance [9]. In addition, although the addition of fluorinated ethylene propylene (FEP) will reduce PEMFC performance, it can increase hydrophobicity and therefore reduce flooding [10].

Due to the beneficial effect on reaction kinetics, catalyst tolerance, heat rejection, and water management, the operation of a PEMFC at a high temperature (>80 °C) is considered to be an effective way to improve fuel cell performance [21–32]. While there are several compelling reasons for operating at a higher temperature, several researchers have studied PEMFC operation at room temperature [33,34], and we decided to operate PEMFCs at 40 °C in this experiment since we plan to apply fuel cells in products that require a low relative humidity. Gasket thickness will also affect performance, and PEMFC performance is optimal when GDL thickness is slightly greater than that of the gasket [20]. We specifically chose a gasket thickness of 0.06 mm in this experiment.

Past research [11–18] indicates PAN fibers need much time and processing before they can be can be transformed into graphite fiber. Graphite fiber has the best structure, followed by carbon fiber, and finally by PAN fiber with the worst structure. In addition, graphite fiber is the most expensive, carbon fiber is second, and PAN fiber is the least expensive. In our previous research [8], the better the structure of the fiber, the greater the conductivity. Graphite fiber has the highest conductivity, followed by carbon fiber and PAN fiber. When commercial carbon fiber paper (such as SGL, TORAY) is used to produce fuel cell electrodes, the first step is to carbonize the carbon fiber at a temperature of 1800 °C or higher to obtain graphite fibers. In our previous study [19,20], we used oxidized carbon fiber felt made from oxidized fibers, which had been carbonized at a temperature of 1000 °C–2500 °C. In this study, we used selectively oxidized fibers of the precursor material, PAN fiber felt, to investigate the relationship between fuel cell performance and fiber diameter.

The ultimate purpose of this study is to increase PEMFC performance and reduce cost by improving GDLs. In particular, we investigate the relationship between fuel cell performance and GDLs produced with different PAN fiber diameters, and the examine the effect of varying the thickness, air permeability, porosity, and surface resistivity of the carbon fiber paper on fuel cell performance. The results obtained are compared with relevant data for GDLs made from commercial carbon paper (Toray TGP-H 030).

2. Experimental parameters

Three different types of PAN fiber felt (supplied by the Industrial Technology Research Institute), denoted as E, H and S, and phenolic resin (supplied by Chang Chun Plastics Co., Ltd.) were used. Methanol solutions with and without 10 wt% phenolic resin was prepared. Each type of PAN felt had different characteristics, including diameter, yard weight, air permeability, and thickness. Type E was produced by electro-spinning and types H and S were both made by melt spinning. Table 1 shows the characteristics of each type of PAN felt.

One set of type E, H, and S PAN fiber felt pieces were immersed in a methanol solution containing 10 wt% phenolic resin, yielding felt types denoted as E-10R, H-10R, and S-10R, which were then baked in an oven at 70 °C for 15 min. Two sets of the same types of PAN fiber felt were also immersed in a methanol solution containing no phenolic resin. One of the sets contained felt types denoted as E–N, H–N, and S–N, and the another set, which was impregnated with FEP in a later step, contained felt types denoted as E-10F, H-10F, and S-10F. All PAN fiber felts were then stabilized at 280 °C in an air atmosphere, creating oxidized fiber felts, before being carbonized at 1000 °C in nitrogen to produce carbon fiber papers. A carbonization temperature of 1000 °C was chosen because we expected that a lower carbonization temperature would reduce the carbon fiber diameter, and thus achieve a better carbon structure. The E-10F, H-10F, and S-10F carbon fiber papers were then impregnated with 10 wt% FEP and sintered in nitrogen at 340 °C.

Table 1
Characteristics of PAN fiber felt and carbon fiber paper.

	Yard weight ($g\ m^{-2}$)	Permeability ($cm^3\ cm^{-2}\ sq^{-1}$)	Thickness (mm)	Fiber volume fraction ($kg\ m^{-3}$)
Type E	32	2	0.3	107
Type E-N(1000 °C)	37	0.9	0.07	529
Type E-10R	77	0	0.2	385
Type E-10F	40	1	0.07	571
Type S	50	30	0.3	167
Type S-N(1000 °C)	41	27	0.16	256
Type S-10R	46	21	0.18	256
Type S-10F	43	22	0.17	253
Type H	35	35	0.2	175
Type H-N(1000 °C)	21	36	0.11	191
Type H-10R	28	29	0.13	215
Type H-10F	22	29	0.11	200
Toray TGP-H 030	44	78	0.11	400

The thickness, air permeability, porosity, and surface resistivity of each piece of carbon fiber paper were measured. The thicknesses of the carbon fiber papers were measured using a Teclock SM-114 thickness tester, and consisted of the average of measurements taken at five random points. Air permeability measurements were performed in accordance with Gurley Model 4110 guidelines using a Gurley Model 4320 m. The porosity of the carbon fiber paper was measured in accordance with ASTM D-570. A Loresta GP MCP-T600 m was used to measure the surface resistivity of the carbon fiber paper in accordance with JIS K 7194. A cold field emission scanning electron microscope was used to observe the surface of the carbon fiber paper.

The carbon fiber paper and the commercial carbon paper (Toray TGP-H 030) were prepared as PEMFC GDLs. Each type of paper was cut into 5 × 5 cm pieces, which were used to make three-layer membrane electrode assemblies (MEAs) containing catalyst-coated membranes (CCM) consisting of Dupont NRE-211. The MEAs were then placed in a fuel cell testing module. Each MEA had an activated area of 25 cm^2, and the bipolar plates consisted of gate-type grooved graphite plates made of highly compacted graphite. The gas flows at the anode (H_2) and the cathode (O_2) were 500 cc min^{-1}, and the gases had a relative humidity of 95%. The temperatures of the anode and cathode were both 40 °C. All single cell operations were performed without external pressurization, and pure humidified hydrogen and pure oxygen were used. The gasket thickness was 0.06 mm.

3. Results and discussion

Fig. 1 shows thickness and surface resistivity curves for different types of carbon fiber paper produced from PAN fiber felt. The commercial carbon paper (Toray TGP-H 030) had a thickness of 0.11 mm. The thicknesses of the E–N, H–N, and S–N paper were 0.07 mm, 0.11 mm, and 0.16 mm, and those of the E-10F, H-10F, and S-10F paper were 0.07 mm, 0.11 mm, and 0.17 mm. Because the FEP formed an extremely thin film-like hydrophobic interface layer on the surface of the carbon fiber paper, impregnation with FEP did not significantly change the thickness of the paper. However, the carbon fiber papers impregnated with 10 wt% phenolic resin were relatively thick. The thicknesses of E-10R, H-10R, and S-10R paper

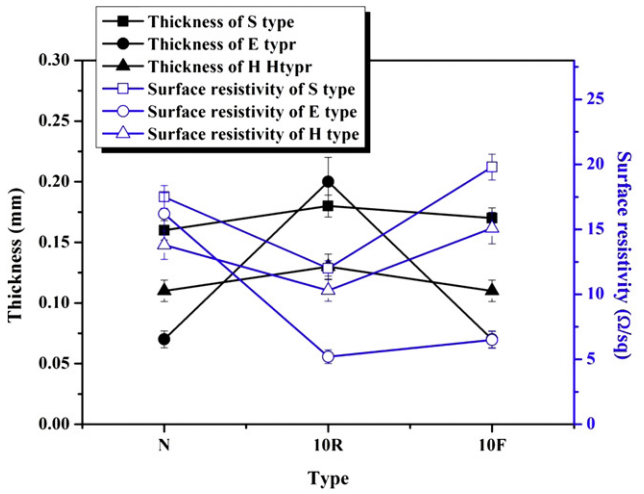

Fig. 1. Thickness and surface resistivity curves for carbon fiber paper with different fiber diameters produced from PAN fiber felt.

were 0.20 mm, 0.13 mm, and 0.18 mm respectively. The voids between the PAN fibers in these types of carbon fiber paper were filled with phenolic resin, which significantly increased their thickness. However, while impregnation with 10 wt% phenolic resin increased the thickness of carbon fiber paper E-10R made by electro-spinning by 0.13 mm, impregnation increased the thickness of both types of carbon fiber paper produced by melt spinning, H-10R and S-10R, by only approximately 0.02 mm. This phenomenon occurs because the type E paper consisted of fine fibers in a dense arrangement. The phenolic resin filled the spaces between the fibers and forced the fibers apart, causing a significant increase in the paper thickness.

The surface resistivity of the Toray TGP-H 030 paper was 0.29 Ω sq^{-1}. Fig. 1 shows the surface resistivity of type S–N was a relatively high 17.5 Ω sq^{-1}, while that of H–N was a relatively low 13.8 Ω sq^{-1} due to the latter type's higher fiber volume fraction. The yard weight of type S–N was 50 g m^{-2} and that of type H–N was 35 g m^{-2}. The thickness of type S–N was 0.3 mm, but of type H–N was only 0.2 mm. Fiber volume fraction is equal to yard weight/thickness, and type S–N thus had a fiber volume fraction of 167 kg m^{-3}, and type H–N had a fiber volume fraction of 175 kg m^{-3}. It can be also observed that, because FEP is non-conducting, impregnation with 10 wt% FEP causes surface resistivity to increase, and, with FEP inside a GDL, surface deposition will increase while the surface conductivity decreases. The surface resistivity of types S-10F and H-10F both increased by roughly 10%, and the relatively small increase of type E-10F can be attributed to the smaller diameter of the carbon fibers. However, after the addition of phenolic resin, the surface resistivity of types S-10R and H-10R both fell sharply by roughly 27%. This phenomenon occurs because electrons are mainly transmitted along the carbon fibers, and the phenolic resin bound to the fibers of the carbon fiber paper provides an effective electron transmission route from fiber to fiber. In the case of E-10R, due the fineness of the carbon fibers, the phenolic resin could bind to the fiber very easily, and caused the surface resistivity to fall by 68%. Moreover, after undergoing stabilization and carbonization, the surface resistivity of the carbon fiber paper increased relative to that of paper which had only been subjected to the addition of phenolic resin.

Fig. 2(a) shows the air permeability curves of carbon fiber paper made from PAN fiber felt. The commercial carbon fiber paper (Toray TGP-H 030) had an air permeability of 78 cm^3 cm^{-2} s^{-1}. When the three types of carbon fiber paper, S, H, and E, had not yet been carbonized and impregnated with phenolic resin, their air permeabilities were 30 cm^3 cm^{-2} s^{-1}, 35 cm^3 cm^{-2} s^{-1} and 2 cm^3 cm^{-2} s^{-1}, respectively. When they had been carbonized at 1000 °C, but not yet impregnated with phenolic resin, the air permeabilities of types S–N, H–N, and E–N were 27 cm^3 cm^{-2} s^{-1}, 36 cm^3 cm^{-2} s^{-1} and 1 cm^3 cm^{-2} s^{-1}, respectively. Type E–N had an extremely low air permeability because it consisted of electro-spun fibers with a diameter of 400 nm, while types S–N and H–N both consisted of melt-spun fibers with a diameter of 1 μm. Type E–N therefore had a low fiber volume fraction number. The small fiber diameter ensured that the fibers were densely packed. Furthermore, due to the low fiber volume fraction of type E–N, a relatively large amount of phenolic resin could be absorbed in the large spaces between the fibers, and the thickness of type E-10R thus increased to 0.20 mm. Fig. 1 shows that compared with types S-10R and H-10R, type E-10R had the greatest increase in its thickness. After impregnation with 10 wt% phenolic resin, types S-10R and H-10R had air permeabilities of 21 cm^3 cm^{-2} s^{-1} and 29 cm^3 cm^{-2} s^{-1}, respectively. Air permeability was significantly in the case of these types because the phenolic resin locked the fibers in a tight arrangement and also filled the spaces between the fibers. Type E-10R's air permeability was negligible due to the great ability of type E carbon fiber paper to absorb phenolic resin. On the other hand, FEP had less effect than phenolic resin on the air permeability of the

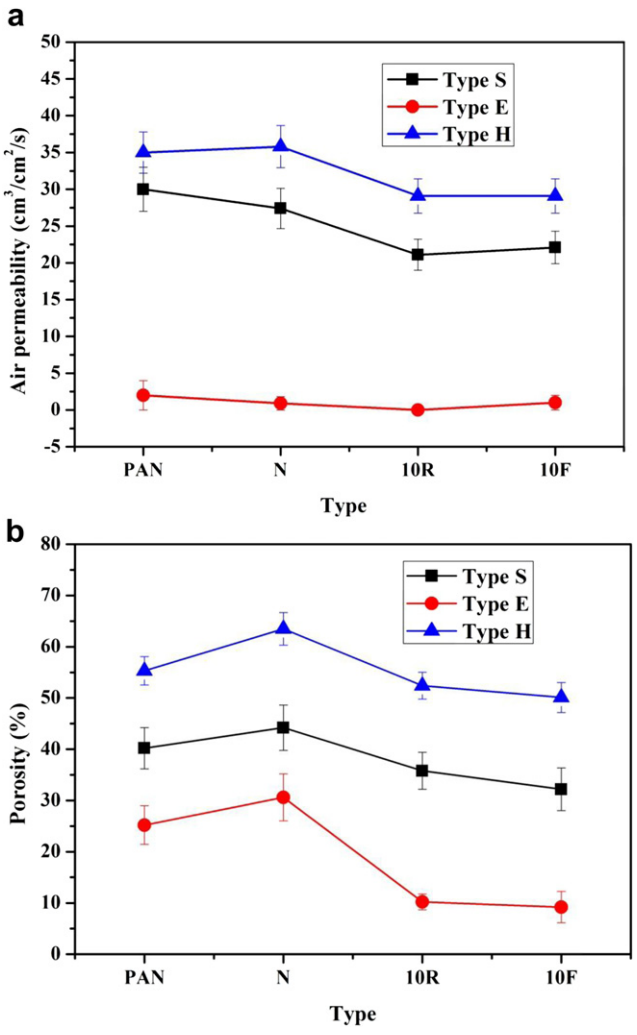

Fig. 2. (a) Air permeability curves for carbon fiber paper made from PAN fiber felt. (b) Porosity curves for carbon fiber paper made from PAN fiber felt.

carbon fiber paper. Even though some was deposited between the fibers, FEP was largely deposited on the surface of the fiber paper. The air permeabilities of types S-10F, H-10F, and E-10F were 22 $cm^3\ cm^{-2}\ s^{-1}$, 29 $cm^3\ cm^{-2}\ s^{-1}$, and 1 $cm^3\ cm^{-2}\ s^{-1}$, respectively.

Fig. 2 (b) shows the porosity curves of carbon fiber paper made from the PAN fiber felt. The Toray TGP-H 030 commercial carbon fiber paper had a porosity of 16%. The porosities of types S, H, and E, before they had been carbonized and impregnated with phenolic resin, were 40%, 55%, and 25%, respectively. When three types of carbon fiber paper had been carbonized at 1000 °C, but phenolic resin had not yet been added, porosities of types S–N, H–N, and E–N were 44%, 64%, and 31%, respectively. Porosity increased in all types of carbon fiber paper because carbonization at 1000 °C caused non-carbon elements to volatilize, creating pores. When phenolic resin was added, the porosities of types S-10R, H-10R, and E-10R were reduced to 36%, 52%, and 10%, respectively, due to the phenolic resin locking the fibers in a tight arrangement and filling the spaces between the fibers. Moreover, due to its high hydrophobicity, FEP reduces the porosity of carbon fiber papers when it is deposited on the surface of the fiber paper. The porosities of types S-10F, H-10F and E-10F were 32%, 50%, and 9%, respectively.

Fig. 3 shows the microstructure of different types of carbon fiber paper produced from PAN fiber felt. Here no resin has been added to the carbon fiber paper, which has been carbonized at 1000 °C. Fig. 3(a) and (e) shows that the fibers in types S–N and H–N have diameters of roughly 1 μm, while the fibers in type E–N are seen to have a diameter of approximately 400 nm in Fig. 3(c), and have an extremely dense arrangement. It can also be seen from Fig. 3 that carbon fiber paper (E–N in Fig. 3 (d)) prepared from carbon fiber felt (E) made using the electro-spinning method displays more tightly interwoven fibers than carbon fiber paper (S–N and H–N in Fig. 3 (b) and (f)) prepared from carbon fiber felt (S, H) made using the spinning method. Because type E–N is so tightly woven, the air permeability and porosity of the resulting carbon fiber paper are low compared with those of types S–N and H–N.

Fig. 4 shows the microstructure of carbon fiber paper produced from PAN fiber felt after impregnation with 10 wt% phenolic resin. These SEM micrographs reveal that, after the impregnation process causes the resin to enter the felt, hot pressing induces the resin to bond to the PAN fibers before high-temperature carbonization transforms the felt into carbon fiber paper. After impregnation with 10 wt% phenolic resin, types S-10R and H-10R had relatively little

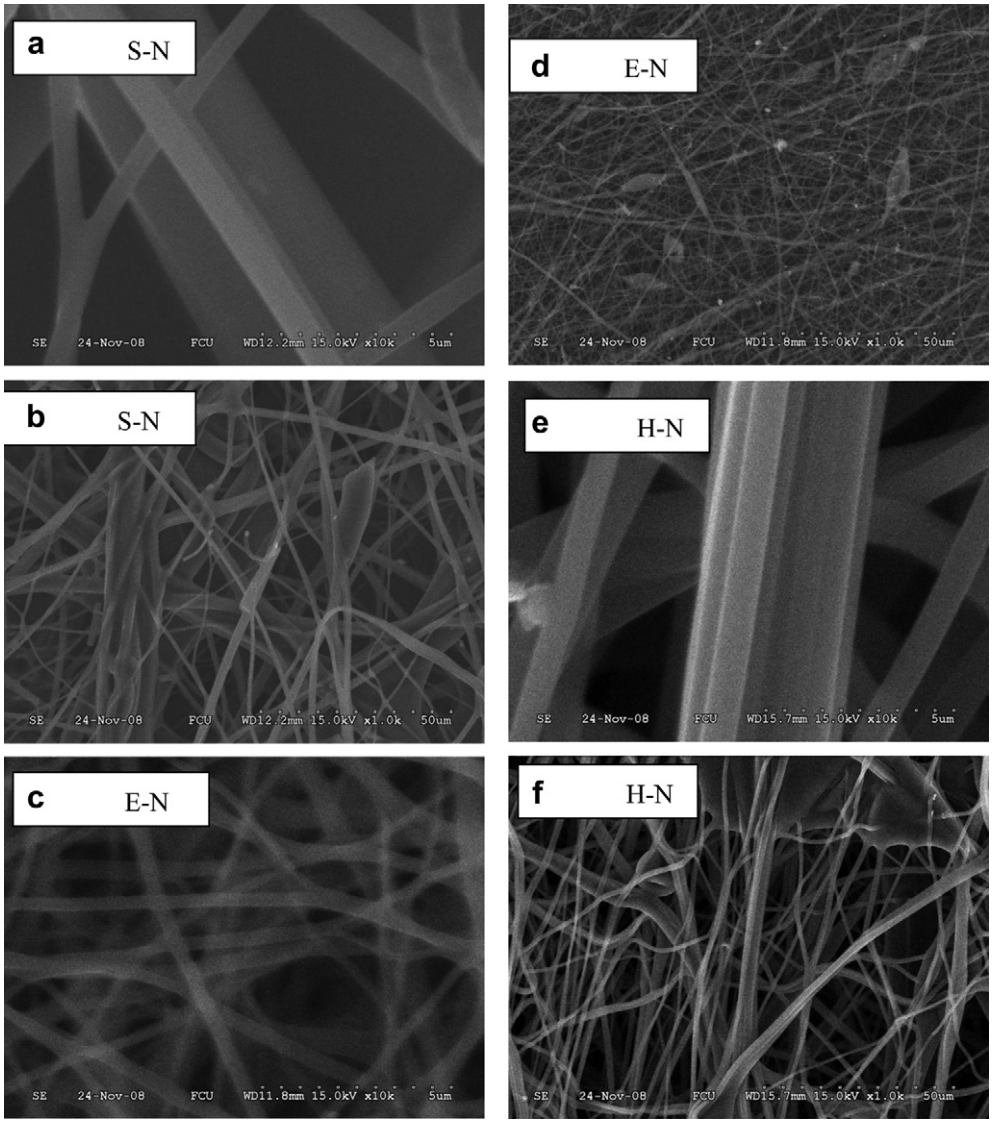

Fig. 3. SEM micrographs of the surface of carbon fiber paper produced from PAN fiber felt: (a) 10,000×, (b) type S–N at 1000×; (c) 10,000×, (d) type E–N at 1000×; (e) 10,000×, (f) type H–N at 1000×.

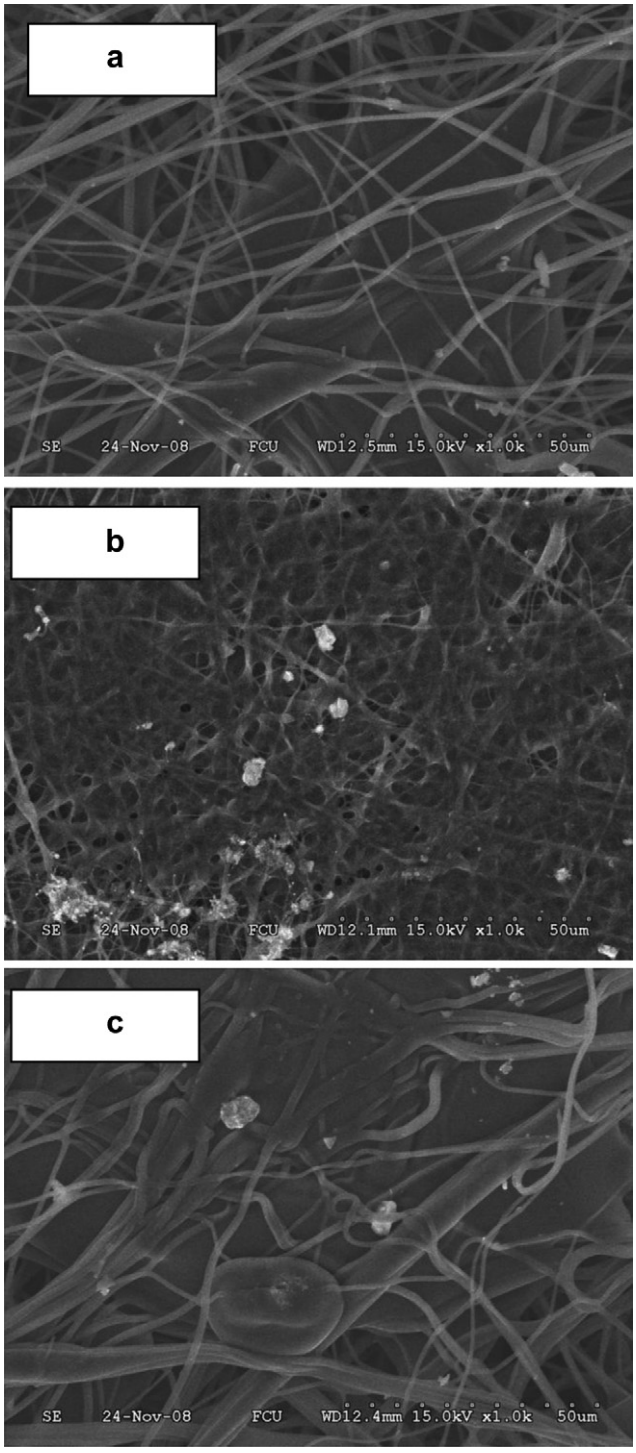

Fig. 4. SEM micrographs (1000×) of the surface of carbon fiber paper produced from PAN fiber felt following impregnation with 10 wt% phenolic resin: (a) type S-10R, (b) type E-10R, and (c) type H-10R.

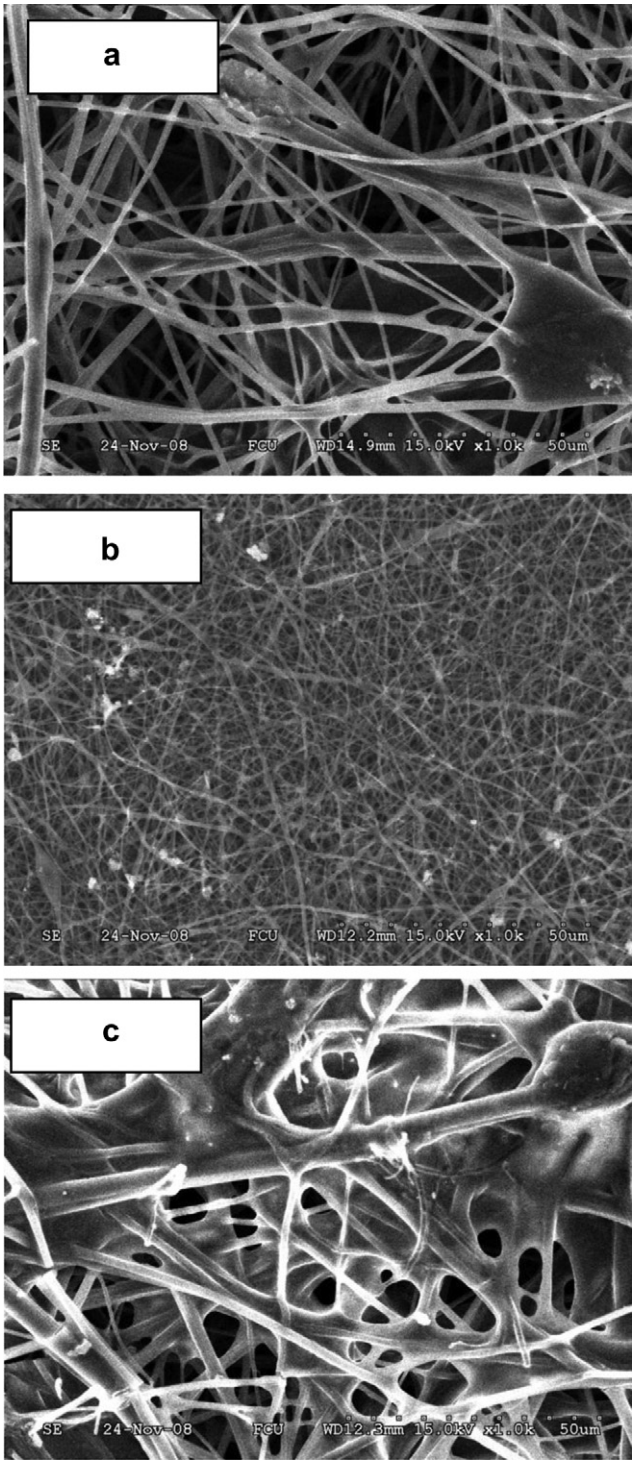

Fig. 5. SEM micrographs (1000×) of the surface of carbon fiber paper produced from PAN fiber felt following impregnation with 10 wt% FEP: (a) type S-10F, (b) type E-10F, and (c) type H-10F.

phenolic resin between their fibers, while type E-10R had a greater amount of phenolic resin between its fibers. As a result, the thickness, surface resistivity, and air permeability of type E-10R changed significantly when phenolic resin was added. Fig. 4 shows that phenolic resin can effectively fill the space between the carbon fibers, resulting in reduced permeability and porosity, but also increases bonding between carbon fibers, so that the surface resistivity decreases and conductivity increases.

Fig. 5 shows the microstructure of carbon fiber paper produced from PAN fiber felt impregnated with 10 wt% FEP. It can be discovered that, after sintering, the FEP forms a hydrophobic film on the surface of the carbon fiber paper. It can also be seen that the FEP is poorly dispersed in the carbon fiber paper, and only part of the paper surface is covered by FEP. In Fig. 5, most FEP has been deposited on the surface of the carbon fibers, whereas the phenolic resin fills the spaces between the carbon fibers. The thickness of

carbon fiber paper had no significant change after adding FEP, which had less effect on thickness than the addition of phenolic resin. Because FEP is a nonconductor, surface resistance increased after the addition of FEP. And because FEP was only deposited on the surface of the carbon fiber, it did not change air permeability. Furthermore, because FEP is highly hydrophobic, the porosity of the paper decreased slightly after FEP was deposited on the surface of the paper. As a consequence, when carbon fiber paper was soaked in 10 wt% FEP, a relatively thick FEP film formed on the surface of types S-10F and H-10F, but only a thin film formed on the surface of type E-10F.

In this article, we used commercial carbon paper (Toray TGP-H 030) to provide baseline data. Carbon fiber paper GDLs were tested in single cells. Polarization curves obtained at a reaction temperature of 40 °C are shown in Fig. 6. Carbon fiber paper was used in the GDLs, and no hydrophobic treatment or micro-electrode layer was applied. It can be seen from Fig. 6 that, when no resin was added, melt spun carbon fiber paper (types S–N and H–N) had a current density of 780 mA cm^{-2} at a load of 0.5 V, while electrospun carbon fiber paper (type E–N) had a current density of 612 mA cm^{-2} at the same load. It can be seen from Fig. 6 that the surface resistivities of types S–N, E–N and H–N were 17.5 Ω sq^{-1}, 16.2 Ω sq^{-1}, and 13.8 Ω sq^{-1}, respectively. Because of the air permeability of type E–N was only 1 cm^3 cm^{-2} s^{-1}, its performance was the worst. Because it had a surface resistivity of 0.29 Ω sq^{-1} and an air permeability of 77.5 cm^3 cm^{-2} s^{-1}, the commercial carbon paper (Toray TGP-H-030) consequently had the best performance. This reveals that although electrospun carbon fiber paper (type E–N) had an air permeability of only 1 cm^3 cm^{-2} s^{-1}, its cell performance was relatively poor, yielding only 612 mA cm^{-2} at a load of 0.5 V. In contrast, melt spun carbon fiber paper (types S–N and H–N) achieved better cell performance.

Fig. 7 shows the result of tests of fuel cells employing carbon fiber paper impregnated with 10 wt% phenolic resin (at a temperature of 40 °C). It can be seen that, while the open circuit potential (OCP) of type E-10R was 0.9 V, melt spun carbon fiber paper that had been impregnated with 10 wt% phenolic resin had an OCP of only 0.75 ± 0.05 V. Since the surface resistivity of type E-10R was 5 Ω sq^{-1}, while types S-10R and H-10R had surface resistivities of 12 Ω sq^{-1} and 10 Ω sq^{-1}, type E-10R had a high open circuit potential. Furthermore, types S-10R, H-10R, and E-10R had current densities of 755, 997, and 120 mA cm^{-2} respectively at a load of 0.5 V. The fact that types S-10R and H-10R had high current densities at a load of 0.5 V can be chiefly attributed to their air permeabilities of 21 cm^3 cm^{-2} s^{-1} and 29 cm^3 cm^{-2} s^{-1}. Because type H-10R had a higher air permeability, its cell performance was better than that of type S-10R. Fig. 7 reveals that although the addition of resin in type H-10R reduced air permeability to 29 cm^3 cm^{-2} s^{-1}, the resin also reduced resistivity to 10 Ω sq^{-1}, which improved battery performance. Since electrospun carbon fiber paper has such a great ability to absorb resin, the addition of resin causes the air permeability to fall to near zero, which prevents gas from reaching the catalyst layer and blocks the transmission of current.

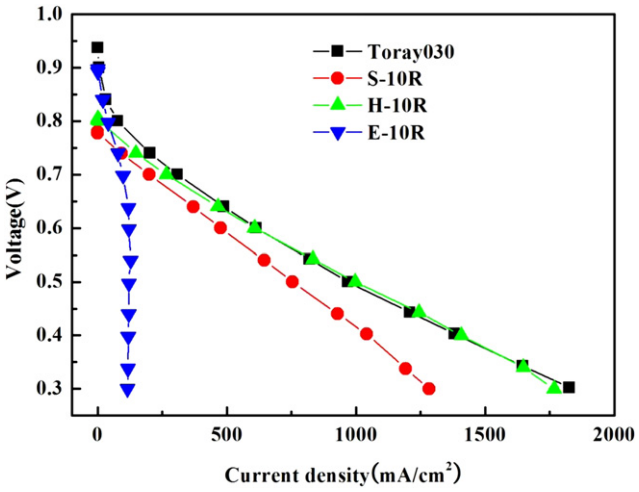

Fig. 7. Fuel cell polarization curves for GDLs prepared using carbon fiber paper prepared from carbon fiber felt impregnated with 10 wt% phenolic resin.

Fig. 8 shows the result of tests of fuel cells employing carbon fiber paper impregnated with 10 wt% FEP and operating at a temperature of 40 °C. Fig. 8 reveals that, when impregnated with 10 wt% FEP, types S-10F, H-10F, and E-10F yielded current densities of 656, 790, and 683 mA cm^{-2} respectively at a load of 0.5 V. The performance of type S-10F was thus relatively poor. Mainly due to the addition of FEP, the surface resistivities of types S-10F, H-10F and E-10F were 20 Ω sq^{-1}, 15 Ω sq^{-1} and 6.5 Ω sq^{-1}. Type S-10F had the highest surface resistivity, which accounted for its poor performance. The surface resistivity of type S increased to 20 Ω sq^{-1}

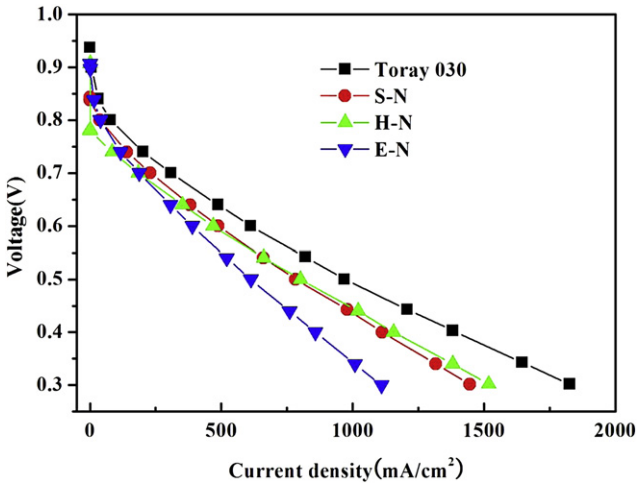

Fig. 6. Fuel cell polarization curves felt at a reaction temperature of 40 °C for GDLs prepared using carbon fiber.

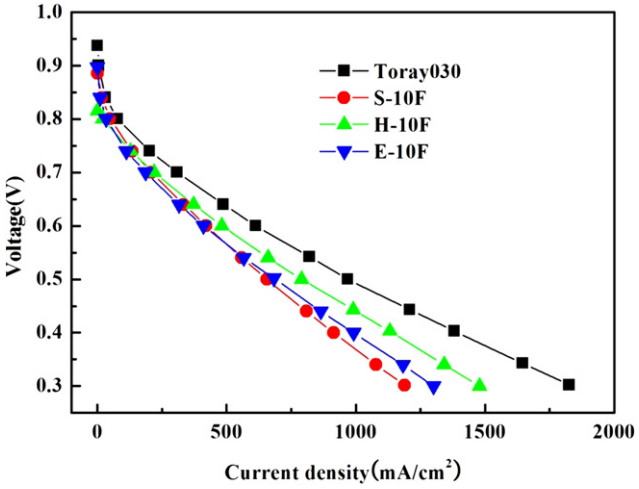

Fig. 8. Fuel cell polarization curves for GDLs prepared using carbon fiber paper prepared from carbon fiber felt impregnated with 10 wt% FEP.

after FEP was added, but even though the surface resistivity increased to $2 \times 10\ \Omega\ sq^{-1}$, the battery still yielded only 656 mA cm^{-2} at a load of 0.5 V.

Impregnation with 10 wt% FEP can increase the hydrophobicity of carbon fiber paper, effectively preventing water or water vapor from being trapped within the GDL. It can be seen from Fig. 8 that, although the performance of melt spun carbon fiber paper can also be improved through impregnation with 10 wt% FEP, the current density of paper produced from electrospun material increased from 612 mA cm^{-2} to 683 mA cm^{-2} at a load of 0.5 V. In the case of melt spun carbon fiber paper, air flow caused by gas in the battery effectively carries water vapor through the GDL; the increase in resistivity caused by the addition of FEP therefore results in relatively poor performance compared with that of paper with no added FEP. Nevertheless, because the air permeability of electrospun carbon fiber paper is relatively low, the outflow of reaction gases cannot carry water vapor, which leads to the accumulation of water vapor within the GDL. Impregnating electrospun carbon fiber paper with FEP increases hydrophobicity, which prevents water vapor from being trapped within the GDL, effectively boosting performance.

4. Conclusions

PAN fiber felts made by melt spinning and electro-spinning method were variously impregnated with phenolic resin and FEP, stabilized at 280 °C, and carbonized at 1000 °C to produce various types of carbon fiber paper, which were then used to make the GDLs for use in PEMFCs. The diameter of the fibers in carbon fiber paper made from electro-spun PAN fiber felt was roughly 400 nm less than those in paper made from melt spun fiber felt. The weave of fibers in type E–N carbon fiber paper, which was made from electric-spun carbon fiber felt, is obviously tighter than that of types S–N and H–N carbon fiber paper, which were made from melt-spun carbon fiber felt. Because of the tight weave of type E–N, its air permeability and porosity were both lower than those of types S–N and H–N. This study found that the addition of phenolic resin increased the thickness of carbon fiber paper produced from electro-spun carbon fiber felt by a factor of 1.8, but increased the thickness of carbon fiber paper made from melt-spun carbon fiber felt by only 20%. Phenolic resin effectively filled the spaces between the carbon fibers and reduced the air permeability and porosity of the carbon fiber paper. It also increased the bonding between the carbon fibers, which reduced the surface resistivity and increased the conductivity of the paper. Although thickness and fiber diameter can be controlled when carbon fiber felt is produced by electrospinning method, this study found that, when the fiber diameter was 400 nm, the pores were too small and the material not suitable for use in PEMFCs. FEP was mostly deposited on the surface of the carbon fiber paper, but it did not fill the space in between the carbon fibers like the phenolic resin. Therefore, after impregnation with FEP, there was no significant change in the thickness of the carbon fiber paper. The surface resistance of the carbon fiber paper increased because FEP is nonconductive. Type E–N carbon fiber paper, which was produced from electro-spun carbon fiber felt, had an extremely low air permeability, which approached 1 $cm^3\ cm^{-2}\ s^{-1}$, and a current density of 612 mA cm^{-2} at a load of 0.5 V. When the gasket thickness was 0.06 mm, type H-10R carbon fiber paper achieved a current density of 996 mA cm^{-2} at a load of 0.5 V, which is comparable with the current density of the commercial carbon fiber paper. Type E-10F carbon fiber paper had a current density of 683 mA cm^{-2} at a load of 0.5 V even though its air permeability was only 1 $cm^3\ cm^{-2}\ s^{-1}$. FEP can therefore facilitate water drainage inside a GDL and allow effective transmission of fuel, especially when the air permeability of the GDL is low.

Acknowledgments

The authors would like to thank the Materials and Chemical Research Laboratories, Industrial Technology Research Institute for financial support.

References

[1] S.D. Fritts, R. Gopal, J. Electrochem. Soc. 140 (1993) 3347.
[2] A. Parthasarathy, S. Srinivasan, J. Appleby, C.R. Martin, J. Electroanal. Chem. 339 (1992) 101.
[3] R.A. Lemons, J. Power Sources 29 (1990) 251.
[4] G. Hoogers, Fuel Cell Technology Handbook, CRC Press LLC, 2002.
[5] M.V. Williams, E. Begg, L. Bonville, H. Russell Kunz, J.M. Fenton, J. Electrochem. Soc. 151 (8) (2004) A1173–A1180.
[6] M.-Z. Wang, New Carbon Mater. 13 (4) (1998) 79.
[7] T.H. Ko, L.C. Huang, J. Appl. Polym. Sci. 70 (1998) 2409–2415.
[8] C.H. Liu, T.H. Ko, W.S. Kuo, H.K. Chou, H.W. Chang, Y.K. Liao, J. Power Sources 186 (2009) 450–454.
[9] M.S.A. Rahaman, A.F. Ismail, A. Mustafa, Polym. Degrad. Stab. 92 (2007) 1421–1432.
[10] A. Gupta, I.R. Harrison, Carbon 34 (1996) 1427–1445.
[11] J.B. Donnet, R.C. Bansal, Carbon Fiber. (1990) 35.
[12] J.B. Donnet, O.P. Bahl, Encycl. Phys. Sci. Technol. 2 (1987) 515.
[13] W. Johnson, L. Philips, W. Watt, U.S. Patent No.412062, (1968).
[14] M.K. Jain, A.S. Abhiraman, J. Mater. Sci. 22 (1978) 278.
[15] E. Fitzer, D.J. Muller, Carbon 13 (1973) 63.
[16] E. Fitzer, W. Frohs, M. Heine, Carbon 24 (1986) 387.
[17] C.H. Liu, T.H. Ko, Y.K. Liao, J. Power Sources 178 (2008) 80–85.
[18] C.H. Liu, T.H. Ko, J.W. Shen, S.I. Chang, S.I. Chang, Y.K. Liao, J. Power Sources 191 (2009) 489–494.
[19] P. Costamagna, S. Srinivasan, J. Power Sources 102 (2001) 242.
[20] P. Costamagna, S. Srinivasan, J. Power Sources 102 (2001) 253.
[21] R.K. Ahluwalia, E.D. Doss, R. Kumar, J. Power Sources 117 (2003) 45.
[22] K.T. Adjemian, S.J. Lee, S. Srinivasan, J. Benziger, A.B. Bocarsly, J. Electrochem. Soc. 149 (2002) A256.
[23] Y.T. Kim, M.K. Song, K.H. Kim, S.B. Park, S.K. Min, H.W. Rhee, Electrochim. Acta 50 (2004) 645.
[24] V. Ramani, H.R. Kunz, J.M. Fenton, J. Membr. Sci. 232 (2004) 31.
[25] C. Yang, P. Costamagna, S. Srinivasan, J. Benziger, A.B. Bocarsly, J. Power Sources 103 (2001) 1.
[26] S. Malhotra, R. Datta, J. Electrochem. Soc. 144 (1997) L23.
[27] Z. Qi, C. He, A. Kaufman, J. Power Sources 111 (2002) 239.
[28] H. Xu, Y. Song, H.R. Kunz, J.M. Fenton, J. Electrochem. Soc. 152 (2005) A1828.
[29] A. Parthasarathy, S. Srinivasan, A.J. Appleby, J. Electrochem. Soc. 139 (1992) 2530.
[30] Y. Song, J.M. Fenton, H.R. Kunz, L.J. Bonville, M.V. Williams, J. Electrochem. Soc. 152 (2005) A539.
[31] Q.F. Li, R.H. He, J.O. Jensen, N.J. Bjerrum, Chem. Mater. 15 (2003) 4896–4915.
[32] K.Y. Chen, A.C.C. Tseung, J. Electroanal. Chem. 451 (1998) 1–4.
[33] C.H. Liu, T.H. Ko, E.C. Chang, H.D. Lyu, Y.K. Liao, J. Power Sources 180 (2008) 276–282.
[34] T.H. Ko, Y.K. Liao, C.H. Liu, New Carbon Mater. 22 (2) (2007) 97–101.